

Electronic Supplementary Information (ESI) for:

**Tetramethoxy-bay-substituted perylene bisimides by  
copper-mediated cross-coupling**

*Pawaret Leowanawat,<sup>a</sup> Agnieszka Nowak-Król,<sup>a</sup> and Frank Würthner\*<sup>a</sup>*

<sup>a</sup> Universität Würzburg, Institut für Organische Chemie & Center for Nanosystems Chemistry,  
Am Hubland, 97074 Würzburg, Germany

E-mail: wuerthner@chemie.uni-wuerzburg.de

## **Table of Contents**

<b>1. Synthesis.....</b>	<b>S1</b>
<b>2. Single Crystal X-ray Analysis.....</b>	<b>S1-S2</b>
<b>3. DFT calculations .....</b>	<b>S2</b>
<b>4. Absorption and emission spectra.....</b>	<b>S3-S5</b>
<b>5. Electrochemistry.....</b>	<b>S5-S6</b>
<b>6. References.....</b>	<b>S7</b>
<b>7. NMR spectra .....</b>	<b>S8-S14</b>

## 1. Synthesis

### Synthesis of compound **7c** via Route A

To a solution of PBI **3** (200 mg, 0.22 mmol) in anhydrous toluene (6.0 mL), anhydrous EtOAc (0.3 mL), CuBr (20 mg, 0.14 mmol), and 25% w/v NaOMe (4.0 mL, 18.5 mmol) in dry MeOH were added. The reaction mixture was refluxed under nitrogen for 30 min. Then the mixture was cooled to room temperature and the reaction was quenched by addition of water and extracted with CH<sub>2</sub>Cl<sub>2</sub>. The organic layer was dried over anhydrous MgSO<sub>4</sub>, filtered and evaporated. The crude product was purified by column chromatography (silica, Et<sub>2</sub>O then hexane to hexane/acetone 4:1) to give **7c** (32 mg, 20%). Characterization data are given in the main text.

## 2. Single Crystal X-ray Analysis

Single crystal X-ray diffraction data for **5** were collected at 100 K on a Bruker D8 Quest Kappa Diffractometer with a Photon100 CMOS detector and multi-layered mirror monochromated CuK<sub>α</sub> radiation. The structures were solved using direct methods, expanded with Fourier techniques and refined with the Shelx software package.<sup>S1</sup> All non-hydrogen atoms were refined anisotropically. Hydrogen atoms were included in the structure factor calculation on geometrically idealized positions.

*Crystal data for **5** (2 C<sub>32</sub>H<sub>28</sub>O<sub>12</sub>· C<sub>7</sub>H<sub>8</sub>): Mr = 1301.22, orange plate, 0.52x0.38x0.05 mm<sup>3</sup>, monoclinic space group P2<sub>1</sub>/c, a = 19.7803(6) Å, α = 90°, b = 8.9250(3) Å, β = 93.0620(10)°, c = 17.1219(5) Å, γ = 90°, V = 3018.37(16) Å<sup>3</sup>, Z = 2, ρ(calcd.) = 1.432 g·cm<sup>-3</sup>, μ = 0.909 mm<sup>-1</sup>, F<sub>(000)</sub> = 1364, GooF(F<sup>2</sup>) = 1.081, R<sub>1</sub> = 0.0448, wR<sup>2</sup> = 0.1018 for I>2σ(I), R<sub>1</sub> = 0.0541, wR<sup>2</sup> = 0.1080 for all data, 5877 unique reflections [θ ≤ 72.265°] with a completeness of 98.9% and 446 parameters, 0 restraints.*

Crystallographic data for the crystal structure of **5** have been deposited in the Cambridge Crystallographic Data Center with CCDC no. 1438126. These data can be obtained free of charge from The Cambridge Crystallographic Data Centre via [www.ccdc.cam.ac.uk/data\\_request/cif](http://www.ccdc.cam.ac.uk/data_request/cif).

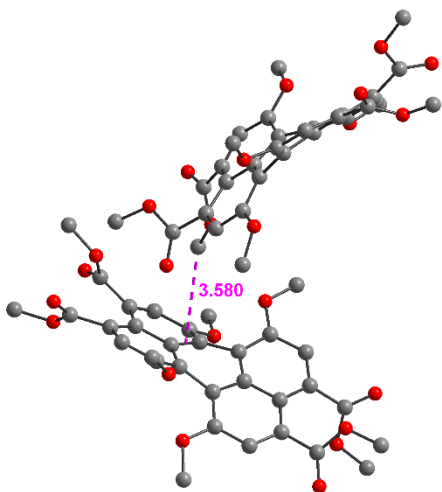


**Fig. S1** Molecular packing of compound **5** in the solid state characterized by CH- $\pi$  interactions. C, grey; O, red. Hydrogen atoms and solvent molecules were omitted for clarity.

### 3. DFT calculations

DFT calculations were performed for a simplified model compound of **7** (imide substituents were replaced by methyl groups) by using the Gaussian 09 program package<sup>S2</sup> with B3-LYP<sup>S3</sup> as a functional and def2-SVP<sup>S4</sup> as a basis set. The structures were geometry optimized, followed by frequency calculations on the optimized structures which confirmed the existence of a minimum. For the starting geometry of **5**, the coordinates of the single crystal structure analysis were used.

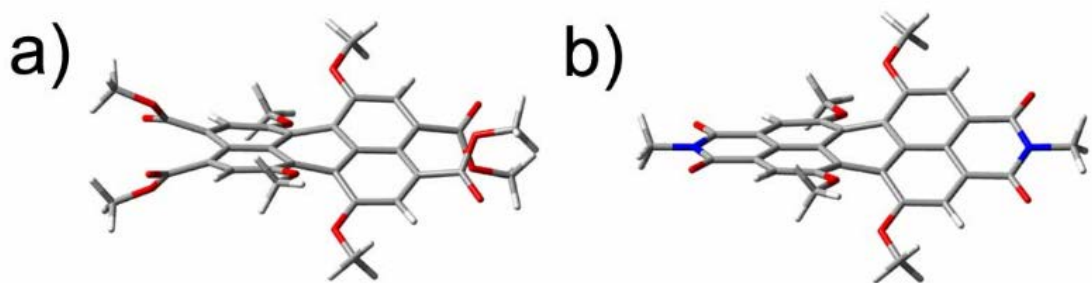


**Fig. S2** Geometry optimized structure (with B3LYP/def2-SVP) of a) **5** and b) **7**. Imide substituents were replaced with methyl groups for simplicity.

#### 4. Absorption and emission spectra

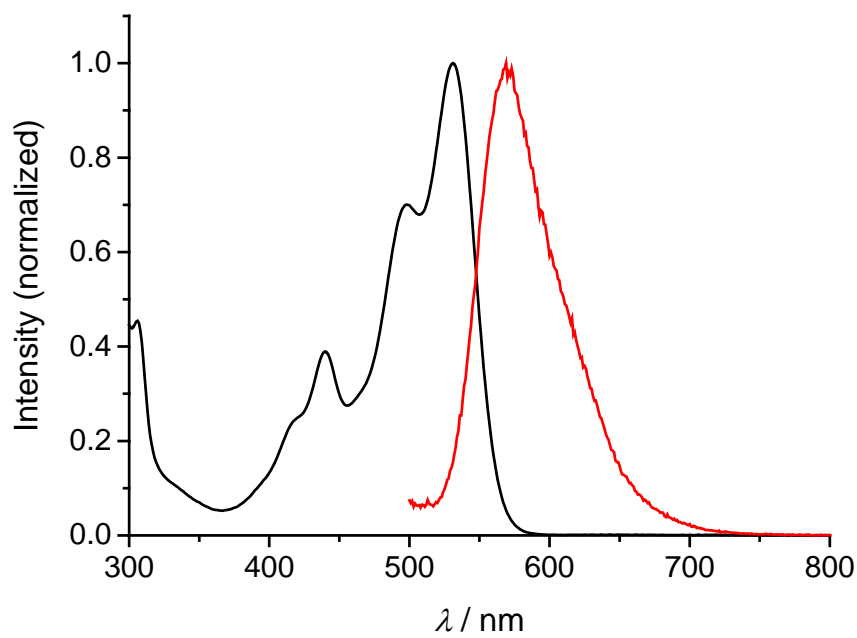


**Fig. S3** Normalized absorption and fluorescence emission spectra of **3** in  $\text{CH}_2\text{Cl}_2$ .

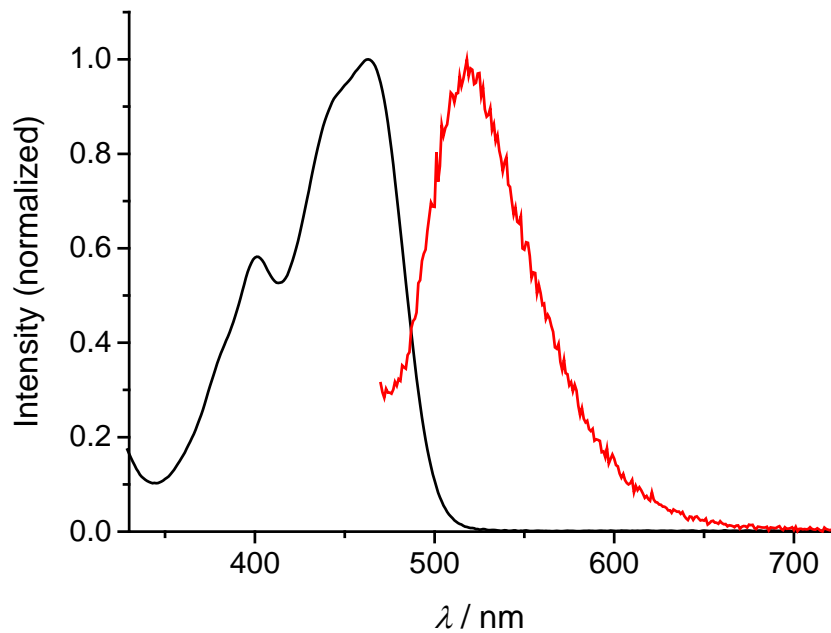


**Fig. S4** Normalized absorption and fluorescence emission spectra of **4** in  $\text{CH}_2\text{Cl}_2$ .

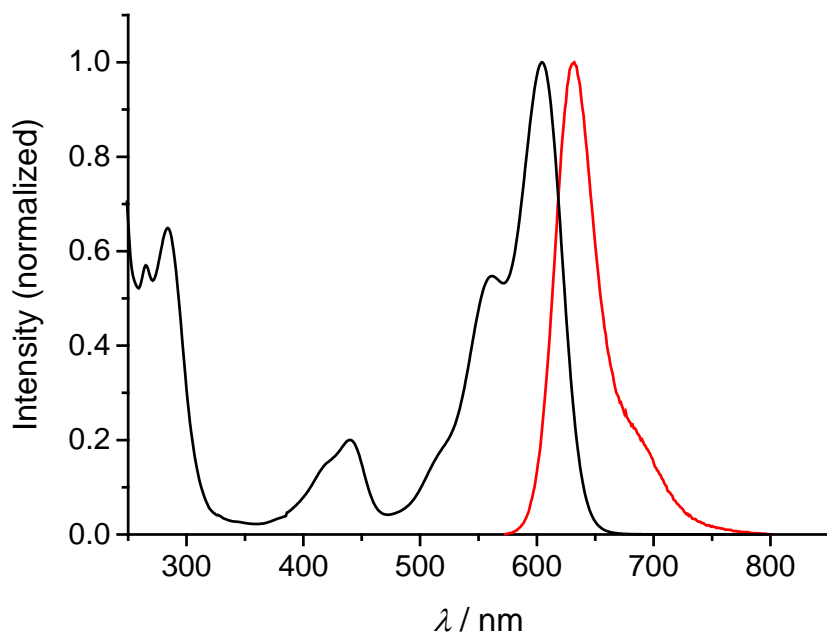


**Fig. S5** Normalized absorption and fluorescence emission spectra of **7b** in  $\text{CH}_2\text{Cl}_2$ .

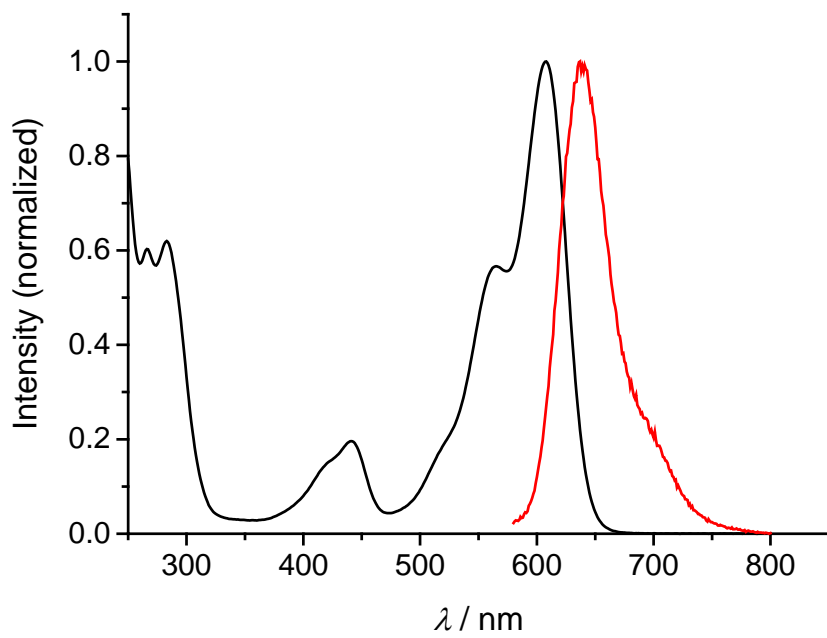


**Fig. S6** Normalized absorption and fluorescence emission spectra of **7c** in  $\text{CH}_2\text{Cl}_2$ .

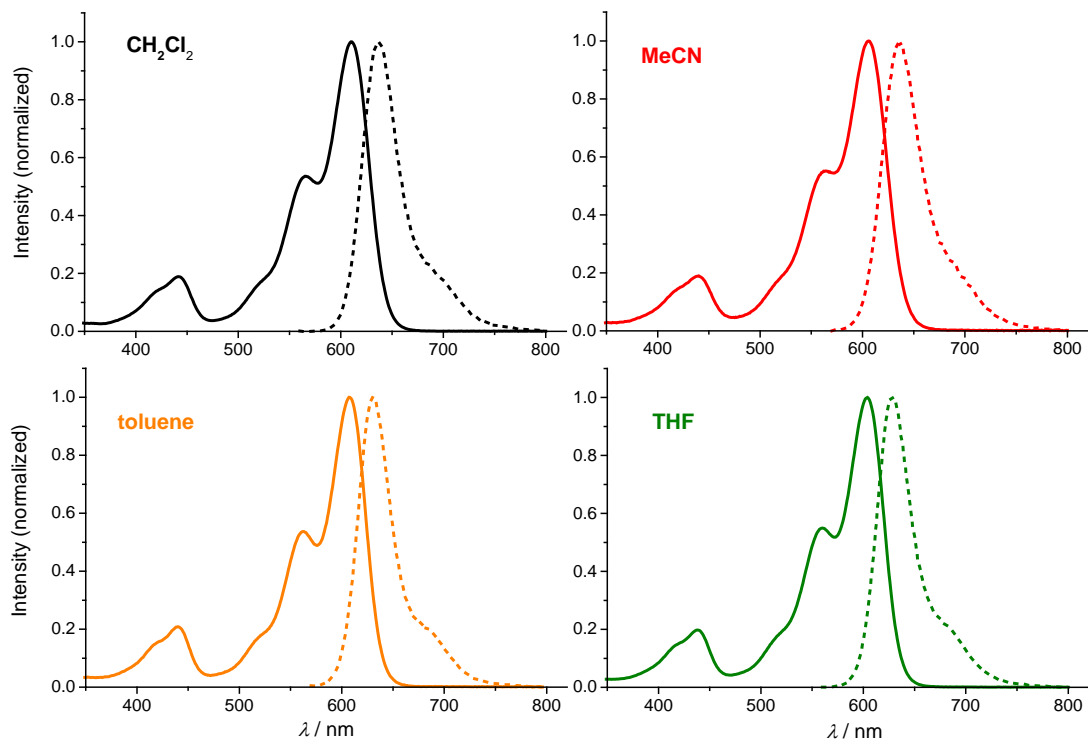


**Fig. S7** Absorption and emission spectra of **7a** in  $\text{CH}_2\text{Cl}_2$  (black lines), MeCN (red lines), THF (green lines), and toluene (orange lines) normalized to the 0-0 transition. Solid and dashed lines depict absorption and emission spectra, respectively.

## 5. Electrochemistry

**Table S1.** Reduction and oxidation potentials of investigated molecules measured in  $\text{CH}_2\text{Cl}_2$  by square-wave voltammetry (SWV) and differential pulse voltammetry (DPV).

Compound	Method	$E$ (Red2) [V]	$E$ (Red1) [V]	$E$ (Ox1) [V]	$E$ (Ox2) [V]
<b>7a</b>	SWV	-1.40	-1.24	+0.66	+1.07
	DPV	-1.40	-1.24	+0.66	+1.06
<b>7b</b>	SWV	-1.44	-1.31	+0.60	+1.05
	DPV	-1.44	-1.30	+0.60	+1.05
<b>9</b>	SWV	-1.35	-1.14	+0.90	+1.22
	DPV	-1.37	-1.15	+0.94	+1.25
<b>8</b>	SWV	-1.27	-1.02	+1.32	-
	DPV	-1.27	-1.03	+1.32	-

<sup>a</sup> Redox potentials vs. ferrocene/ferrocenium ( $\text{Fc}/\text{Fc}^+$ ) in  $\text{CH}_2\text{Cl}_2$  solutions, using  $\text{Bu}_4\text{NPF}_6$  (0.1 M) as a supporting electrolyte.

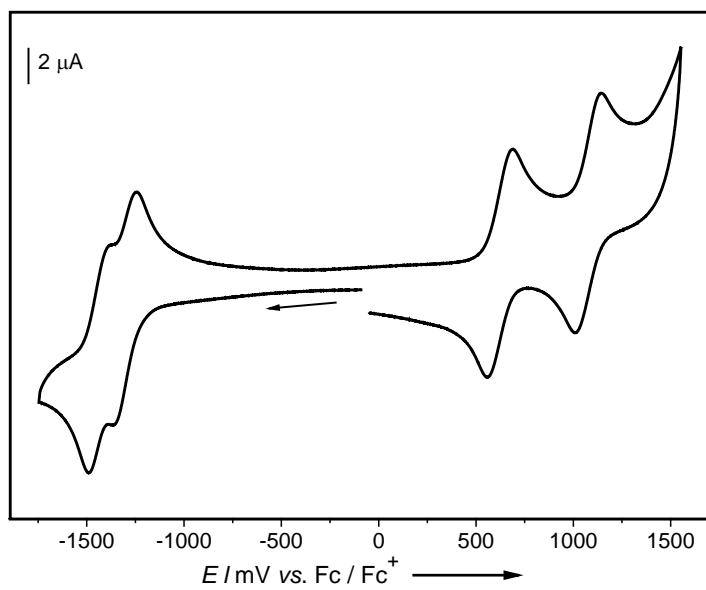


**Fig. S8** Cyclic voltammogram of **7b** ( $3.2 \times 10^{-4}$  M) in  $\text{CH}_2\text{Cl}_2$  solution of  $\text{Bu}_4\text{NPF}_6$  (0.1 M) at a scan rate of  $100 \text{ mV s}^{-1}$ . The measurement was calibrated with an internal standard (ferrocene/ferrocenium).

## 6. References

- <sup>S1</sup> G. M. Sheldrick, *Acta Crystallogr. A*, 2008, **64**, 112.
- <sup>S2</sup> Gaussian 09, Revision D.01, M. J. Frisch, G. W. Trucks, H. B. Schlegel, G. E. Scuseria, M. A. Robb, J. R. Cheeseman, G. Scalmani, V. Barone, B. Mennucci, G. A. Petersson, H. Nakatsuji, M. Caricato, X. Li, H. P. Hratchian, A. F. Izmaylov, J. Bloino, G. Zheng, J. L. Sonnenberg, M. Hada, M. Ehara, K. Toyota, R. Fukuda, J. Hasegawa, M. Ishida, T. Nakajima, Y. Honda, O. Kitao, H. Nakai, T. Vreven, J. A. Jr. Montgomery, J. E. Peralta, F. Ogliaro, M. Bearpark, J. J. Heyd, E. Brothers, K. N. Kudin, V. N. Staroverov, T. Keith, R. Kobayashi, J. Normand, K. Raghavachari, A. Rendell, J. C. Burant, S. S. Iyengar, J. Tomasi, M. Cossi, N. Rega, J. M. Millam, M. Klene, J. E. Knox, J. B. Cross, V. Bakken, C. Adamo, J. Jaramillo, R. Gomperts, R. E. Stratmann, O. Yazyev, A. J. Austin, R. Cammi, C. Pomelli, J. W. Ochterski, R. L. Martin, K. Morokuma, V. G. Zakrzewski, G. A. Voth, P. Salvador, J. J. Dannenberg, S. Dapprich, A. D. Daniels, O. Farkas, J. B. Foresman, J. V. Ortiz, J. Cioslowski and D. J. Fox, Gaussian, Inc., Wallingford CT, 2013.
- <sup>S3</sup> a) A. D. Becke, *Phys. Rev. A*, 1988, **38**, 3098; b) C. Lee, W. Yang and R. G. Parr, *Phys. Rev. B*, 1988, **37**, 785-789; c) A. D. Becke, *J. Chem. Phys.*, 1993, **98**, 5648.
- <sup>S4</sup> F. Weigand and R. Ahlrichs, *Phys. Chem. Chem. Phys.*, 2005, **7**, 3297.

## 7. NMR spectra

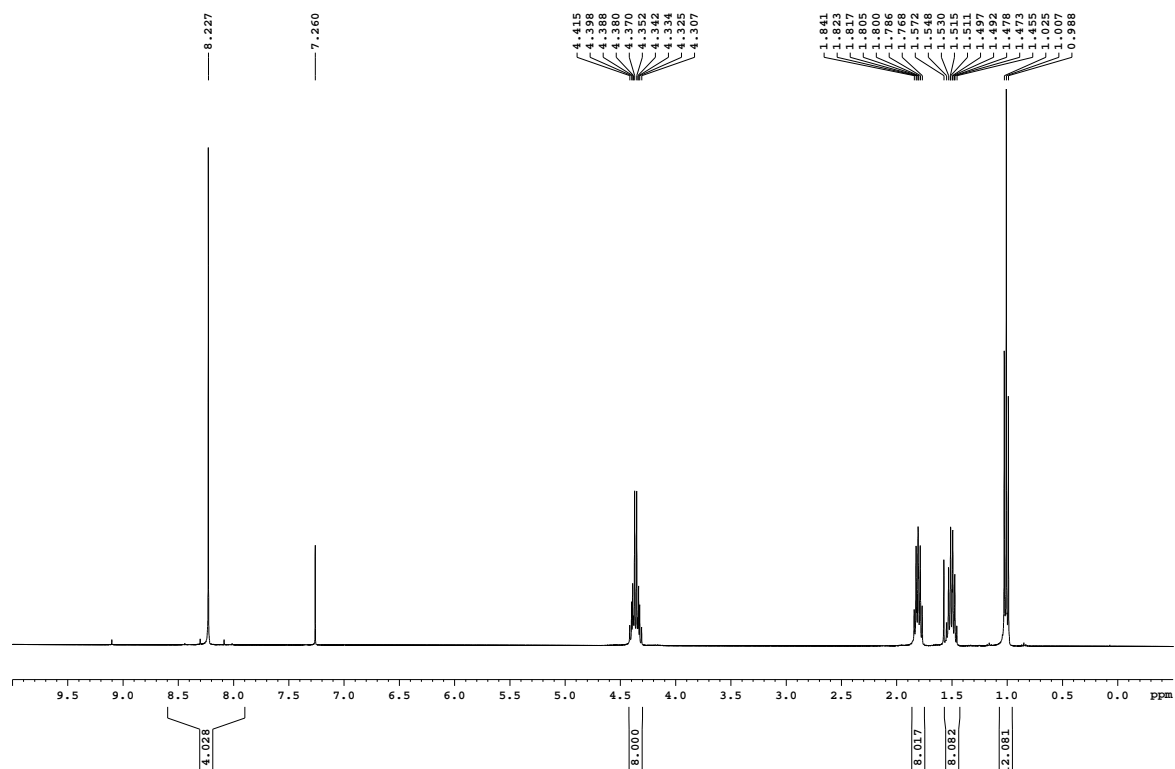


**Fig. S9** <sup>1</sup>H NMR spectrum of **4** (400 MHz, CDCl<sub>3</sub>, 25 °C).

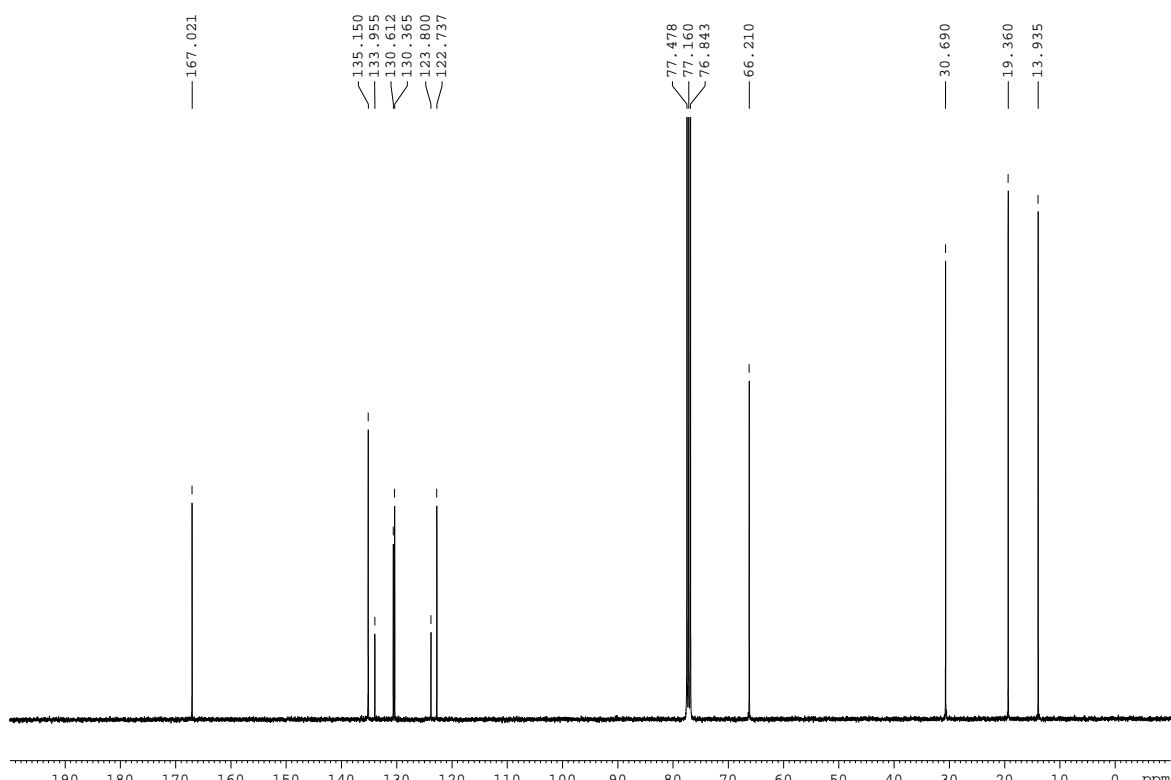


**Fig. S10** <sup>13</sup>C NMR spectrum of **4** (101 MHz, CDCl<sub>3</sub>, 25 °C).

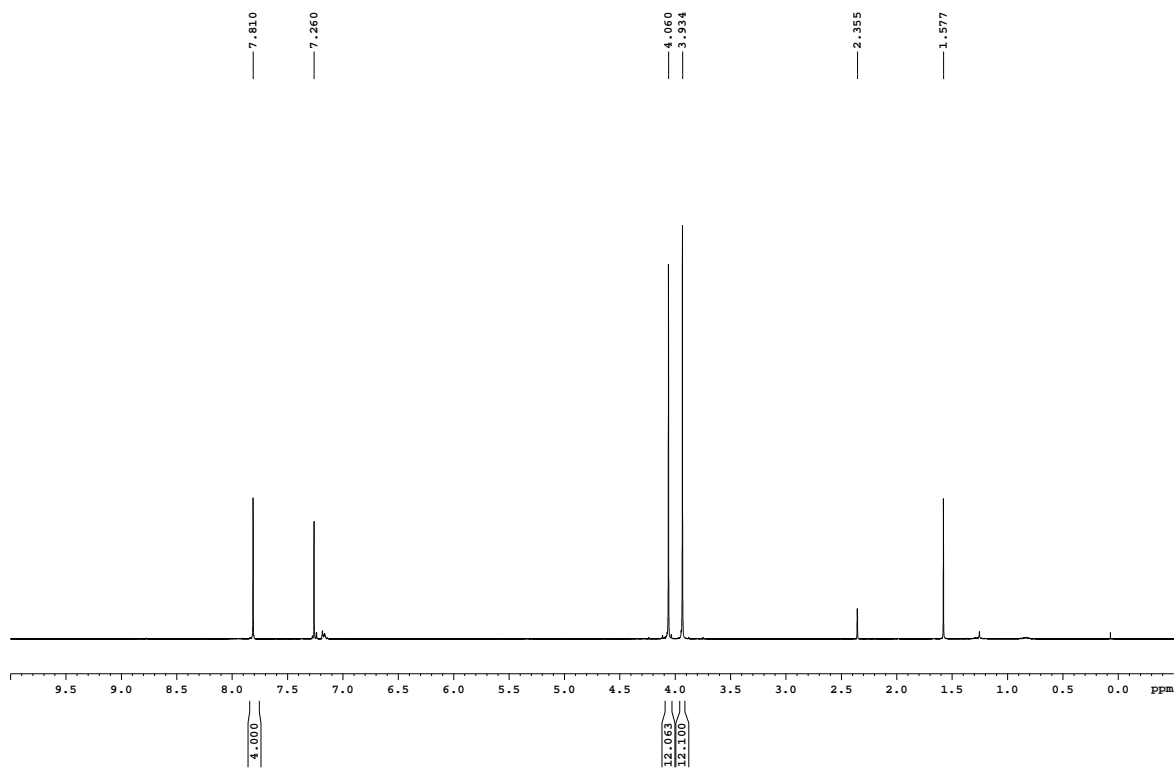


**Fig. S11** <sup>1</sup>H NMR spectrum of **5** (400 MHz, CDCl<sub>3</sub>, 25 °C).

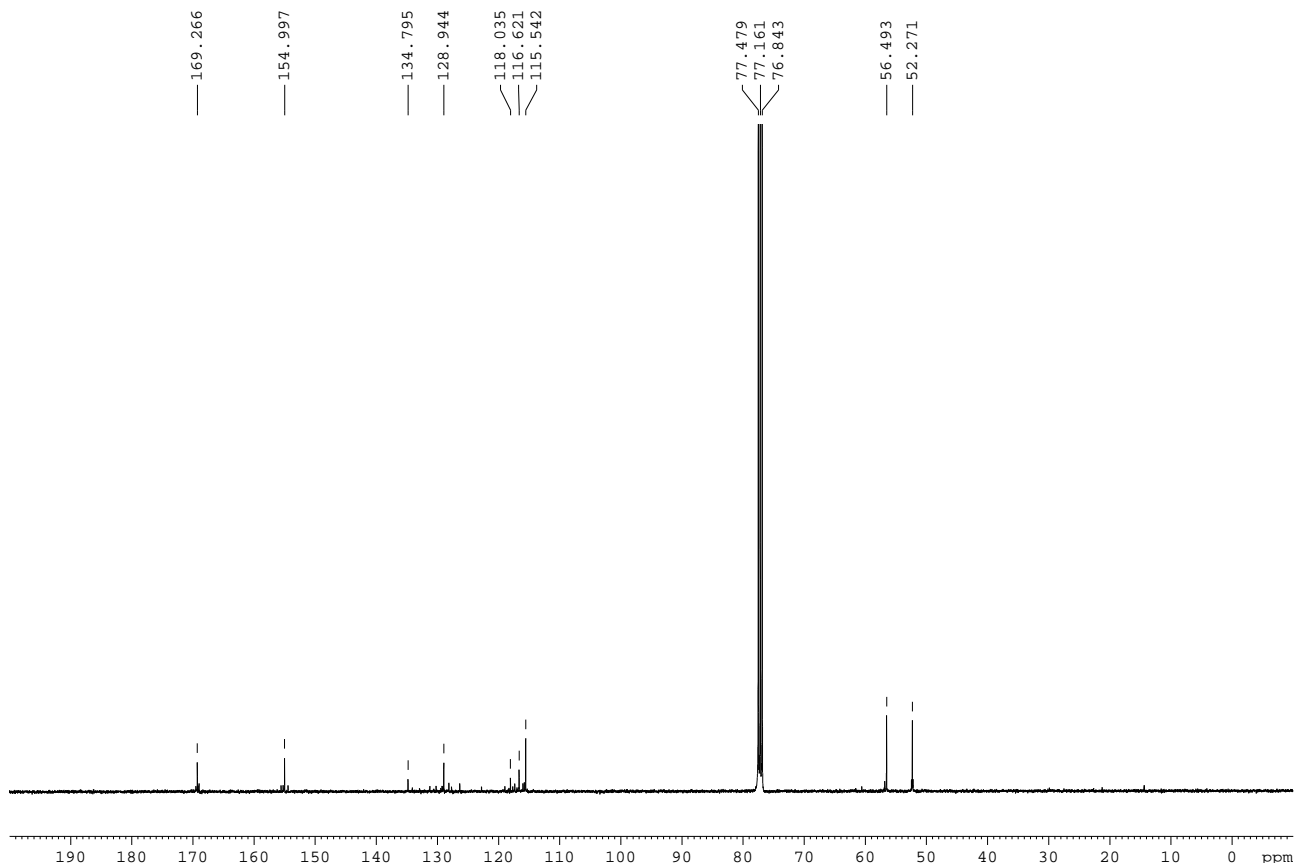


**Fig. S12** <sup>13</sup>C NMR spectrum of **5** (101 MHz, CDCl<sub>3</sub>, 25 °C).

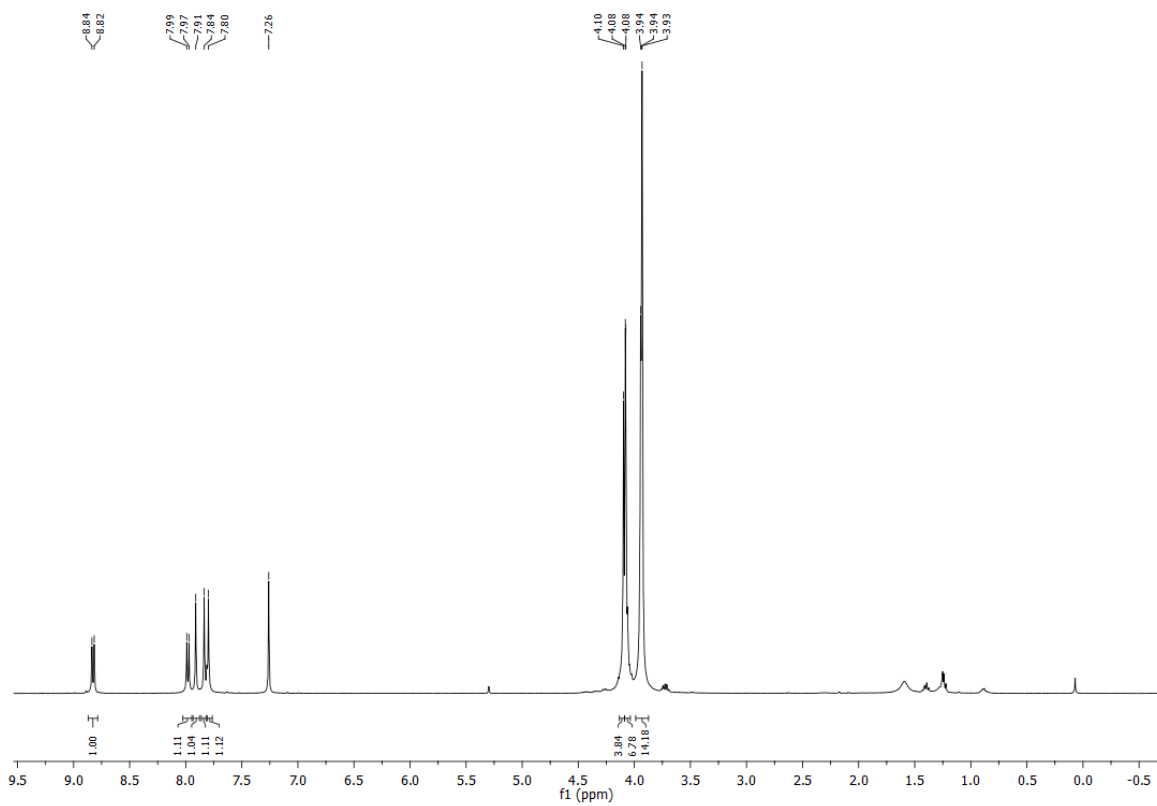


**Fig. S13** <sup>1</sup>H NMR spectrum of **5'** (400 MHz, CDCl<sub>3</sub>, 25 °C).

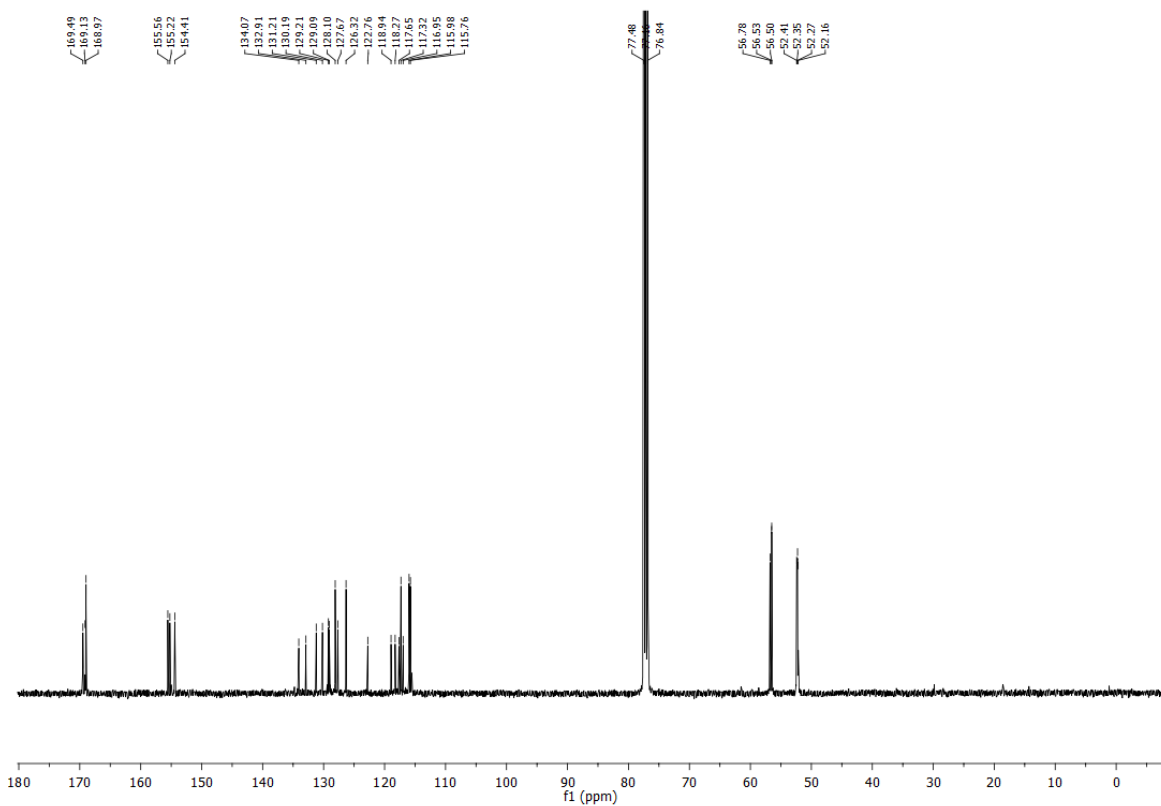


**Fig. S14** <sup>13</sup>C NMR spectrum of **5'** (101 MHz, CDCl<sub>3</sub>, 25 °C).

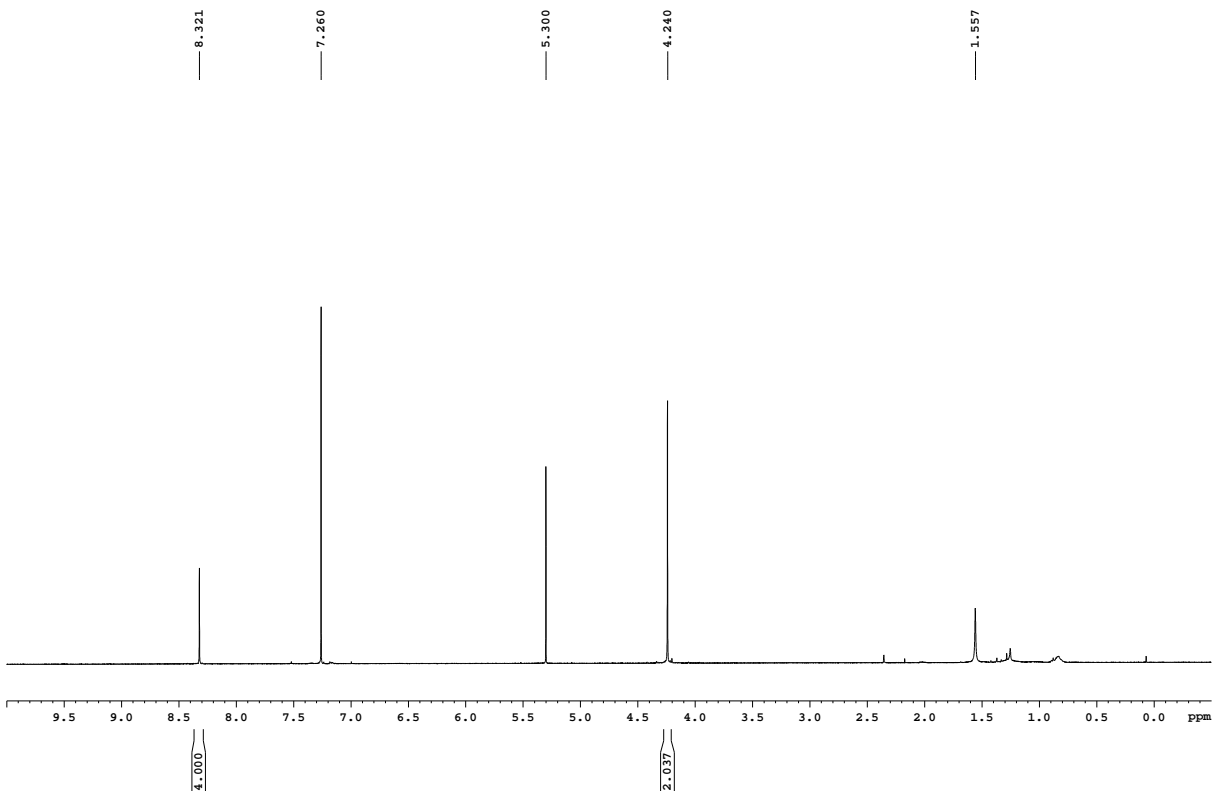


**Fig. S15** <sup>1</sup>H NMR spectrum of **6** (400 MHz, CDCl<sub>3</sub>, 25 °C).

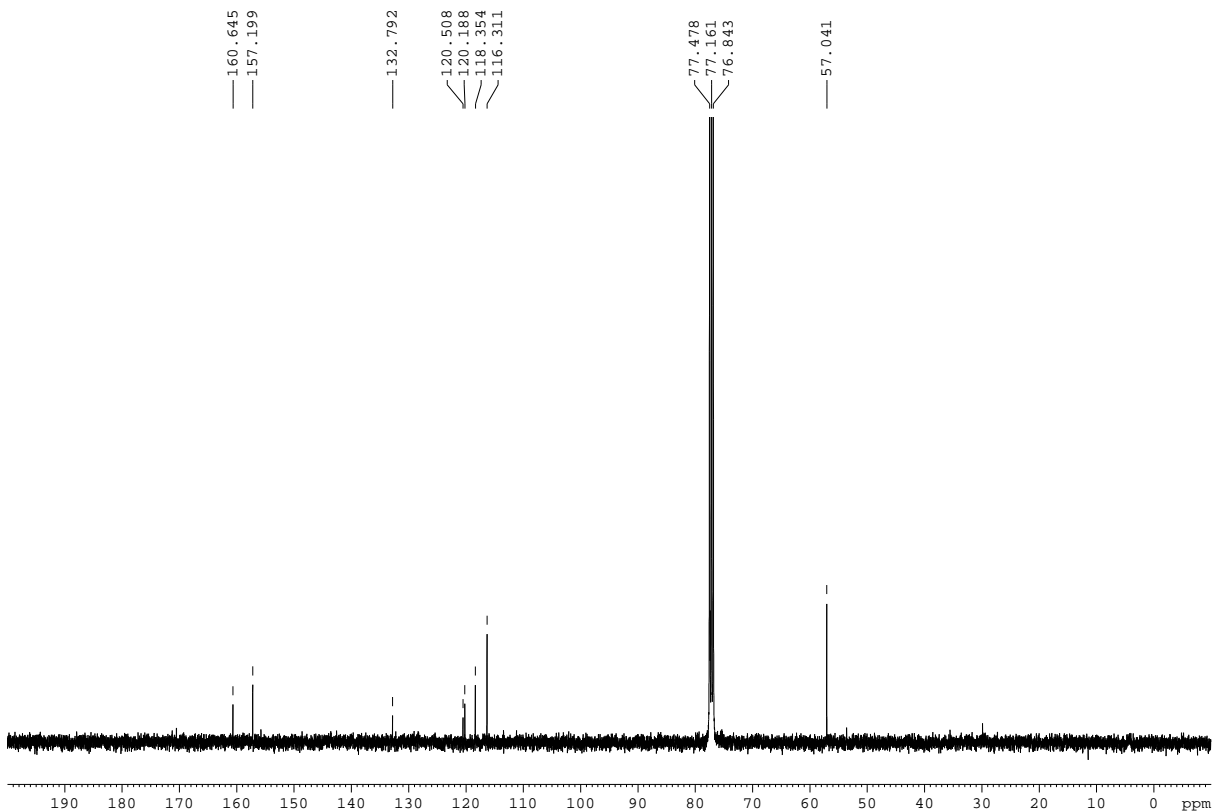


**Fig. S16** <sup>13</sup>C NMR spectrum of **6** (101 MHz, CDCl<sub>3</sub>, 25 °C).

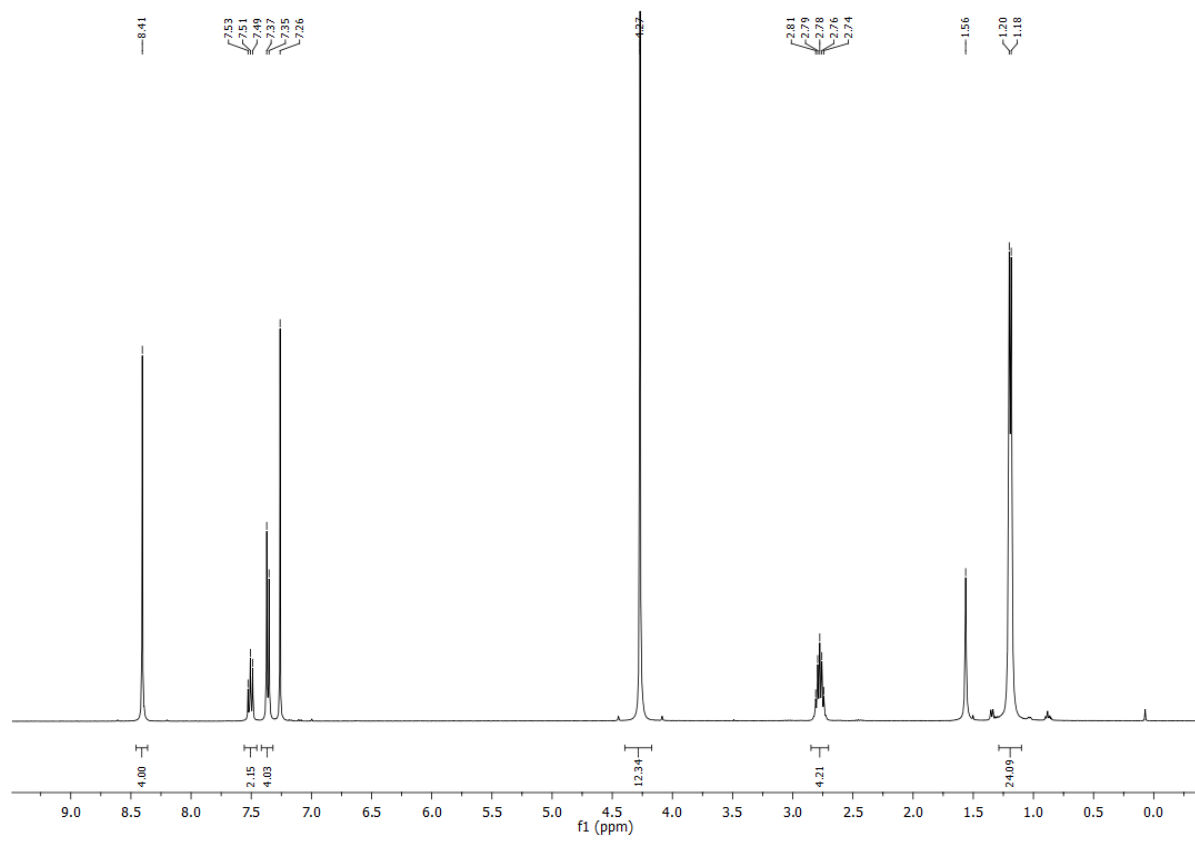


**Fig. S17**  $^1\text{H}$  NMR spectrum of **7a** (400 MHz,  $\text{CDCl}_3$ , 25 °C).

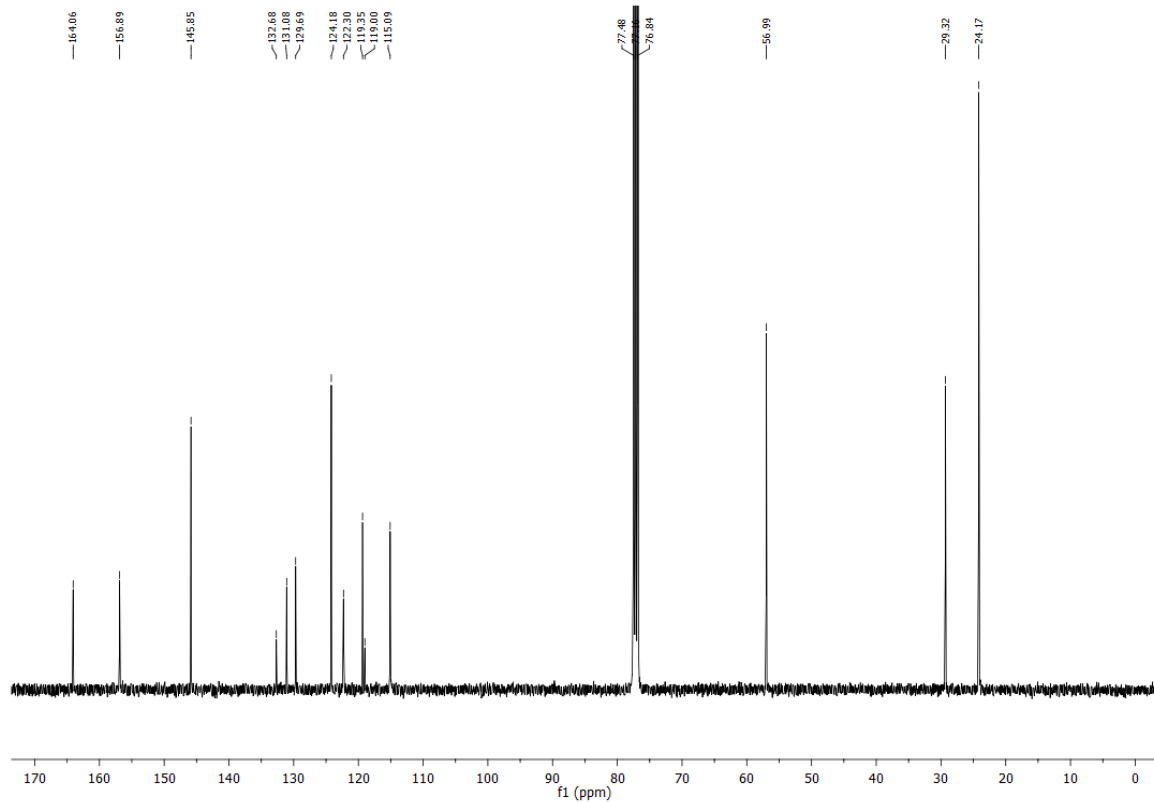


**Fig. S18**  $^{13}\text{C}$  NMR spectrum of **7a** (101 MHz,  $\text{CDCl}_3$ , 25 °C).

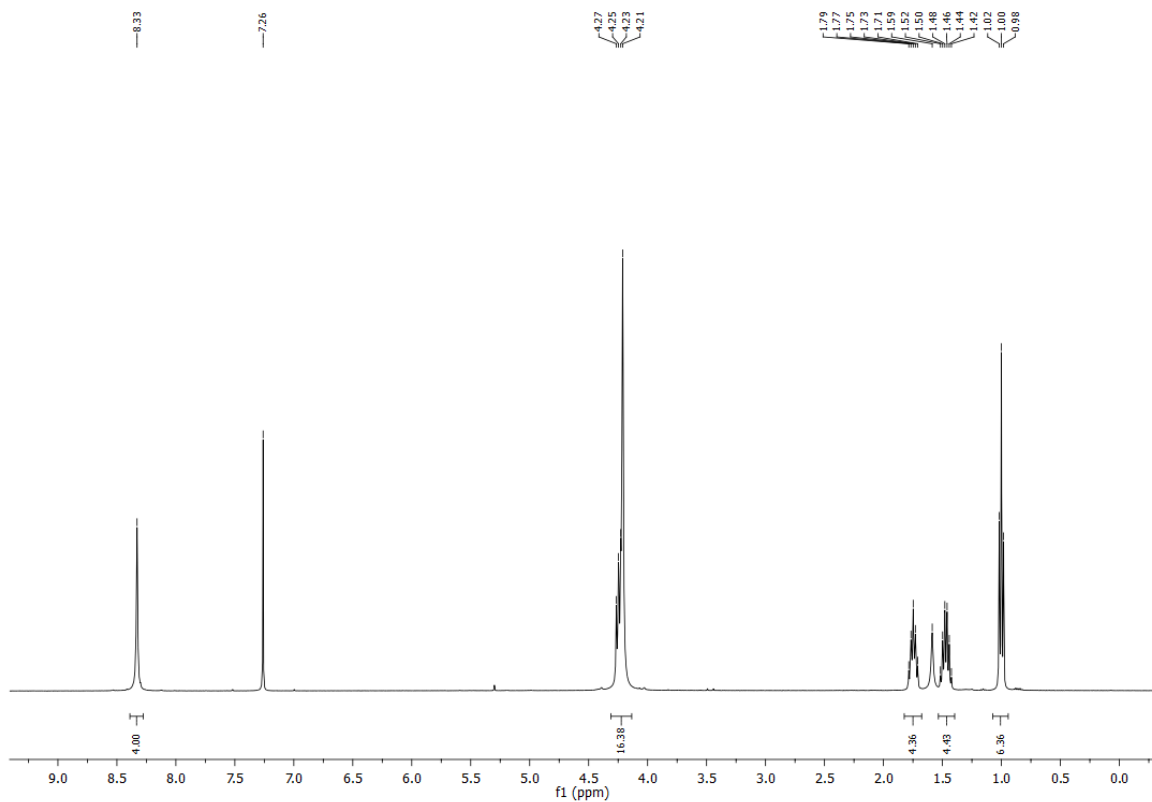


**Fig. S19**  $^1\text{H}$  NMR spectrum of **7b** (400 MHz,  $\text{CDCl}_3$ , 25 °C).

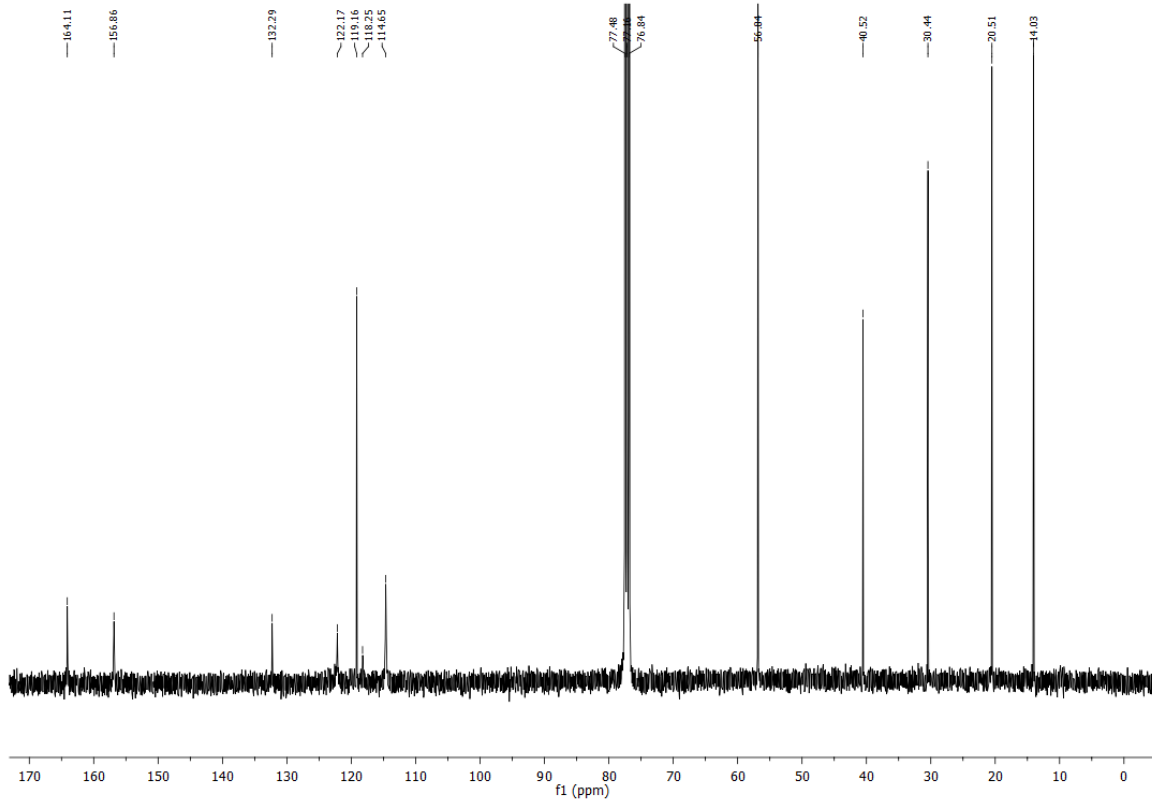


**Fig. S20**  $^{13}\text{C}$  NMR spectrum of **7b** (101 MHz,  $\text{CDCl}_3$ , 25 °C).

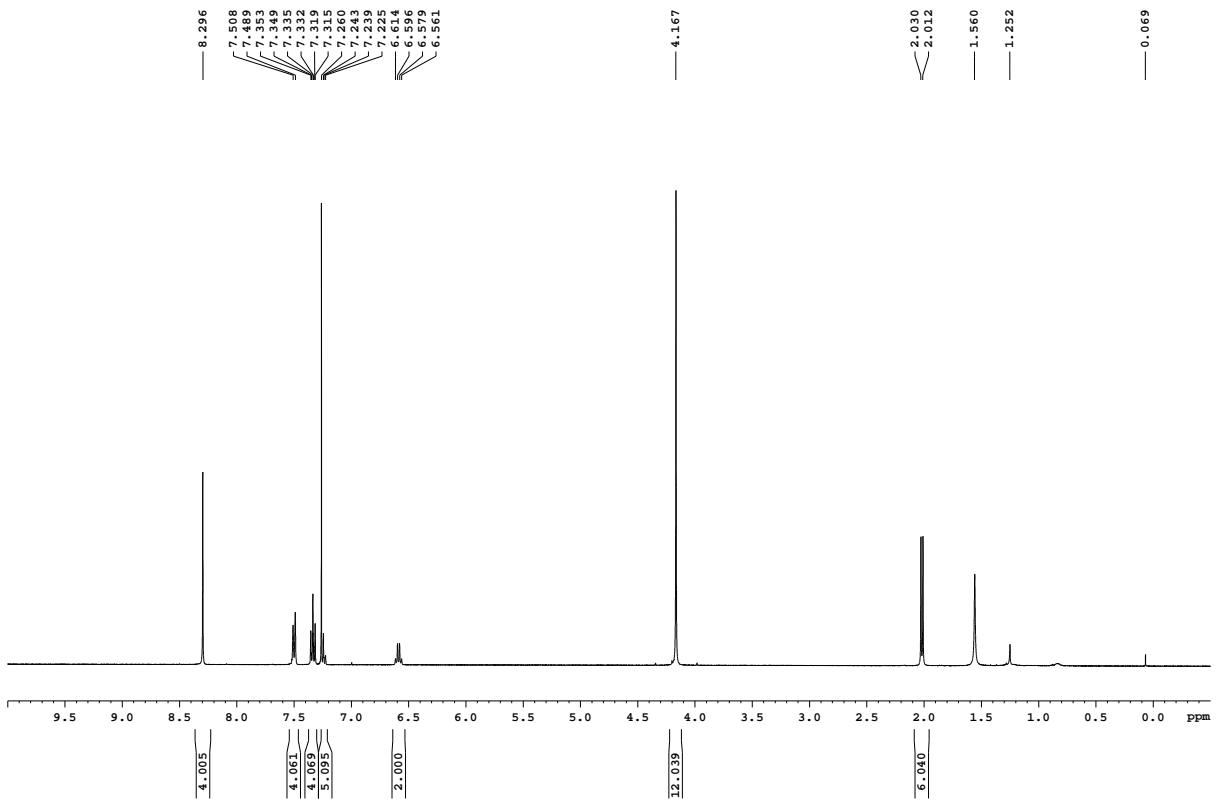


**Fig. S21**  $^1\text{H}$  NMR spectrum of **7c** (400 MHz,  $\text{CDCl}_3$ , 25 °C).

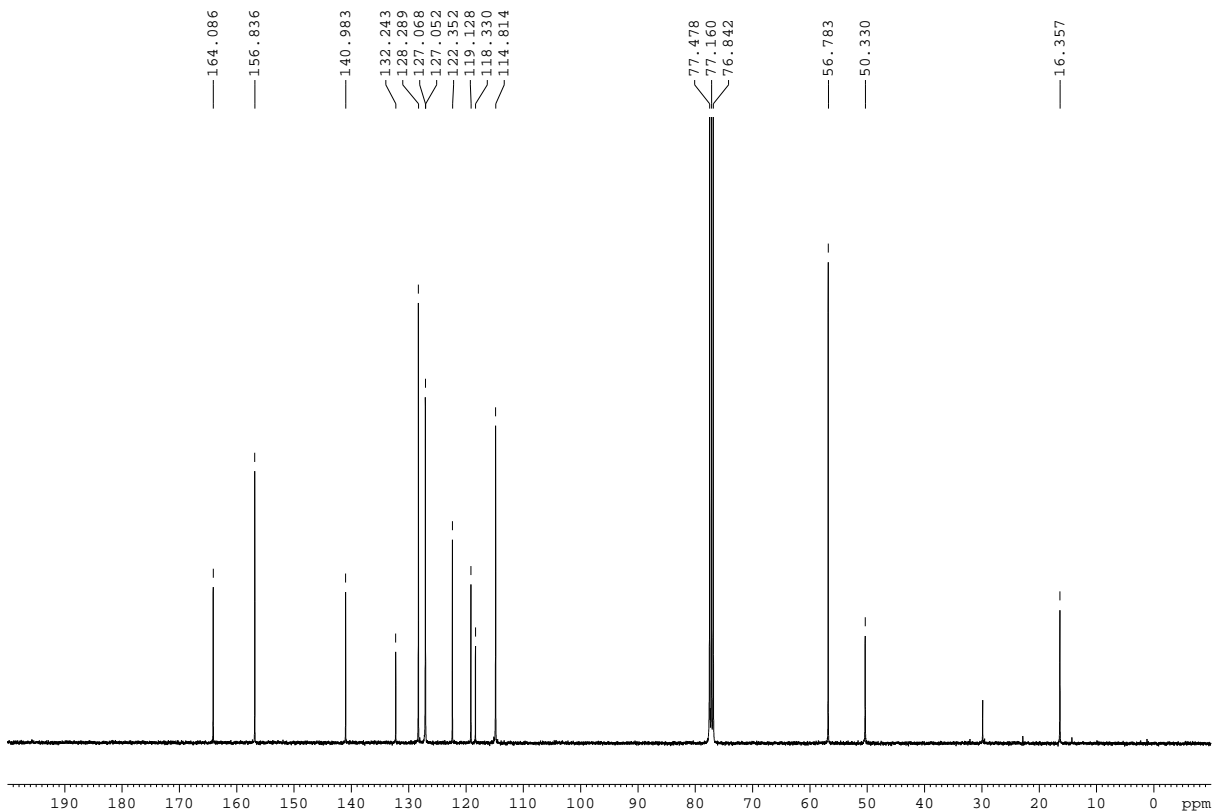


**Fig. S22**  $^{13}\text{C}$  NMR spectrum of **7c** (101 MHz,  $\text{CDCl}_3$ , 25 °C).